

Kinematic Flow and the Emergence of Time

Nima Arkani-Hamed,¹ Daniel Baumann,^{2,3,4} Aaron Hillman,^{5,6}
Austin Joyce,^{7,8} Hayden Lee,⁸ and Guilherme L. Pimentel⁹

¹*Institute for Advanced Study, Princeton, NJ 08540, USA*

²*Leung Center for Cosmology and Astroparticle Physics, Taipei 10617, Taiwan*

³*Center for Theoretical Physics, National Taiwan University, Taipei 10617, Taiwan*

⁴*Institute of Physics, University of Amsterdam, Amsterdam, 1098 XH, The Netherlands*

⁵*Walter Burke Institute for Theoretical Physics, Caltech, Pasadena, CA 91125, USA*

⁶*Department of Physics, Jadwin Hall, Princeton University, NJ 08540, USA*

⁷*Department of Astronomy and Astrophysics, University of Chicago, Chicago, IL 60637, USA*

⁸*Kavli Institute for Cosmological Physics, University of Chicago, Chicago, IL 60637, USA*

⁹*Scuola Normale Superiore and INFN, Piazza dei Cavalieri 7, 56126, Pisa, Italy*

Perhaps the most basic question we can ask about cosmological correlations is how their strength changes as we smoothly vary kinematic parameters. The answer is encoded in differential equations that govern this evolution in kinematic space. In this Letter, we introduce a new perspective on these differential equations. We show that, in the simplified setting of conformally coupled scalars in a general FRW spacetime, the equations for arbitrary tree-level processes can be obtained from a small number of simple combinatorial rules. While this “kinematic flow” is defined purely in terms of boundary data, it reflects the physics of bulk time evolution. The unexpected regularity of the equations suggests the existence of an autonomously defined mathematical structure from which cosmological correlations, and the time evolution of the associated spacetime, emerge.

Cosmology gives us the strongest motivations to replace the seemingly foundational notion of spacetime with deeper, and likely more abstract, principles. From the breakdown of Einstein gravity coupled to matter near the Big Bang singularity, to the profound mysteries associated with the accelerated expansion of our Universe, it is cosmology that most powerfully calls for an overhaul of our description of the laws of Nature, jettisoning the phrase “time evolution” from the vocabulary of fundamental physics at the deepest level, and instead seeing the concept of time emerge as an extremely useful approximation when this becomes possible.

It is also suggestive that our actual observations of the Universe are static, correlating measurements at different positions in the late Universe. We introduce a cosmological history to give a rational accounting of these spatial patterns, but ultimately the notion of “cosmological time” is an auxiliary one, not present in the observables themselves. There should therefore be a description of the same physics that focusses only on the observed static correlations and in which time evolution becomes a derived concept.

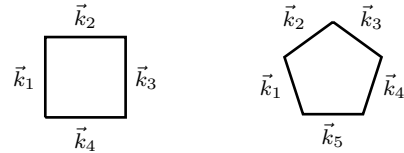
Another motivation for reformulating cosmological perturbation theory in a way that dispenses with explicit evolution in time is that the standard “time-centered” computations are very complex. This complexity can be traced to the time integrals over interactions in the quantum-mechanical sum over histories, and it likely conceals fascinating new physical and mathematical structures underlying cosmological correlators.

For several years, these developments have been calling for the formulation of a radically new, “timeless” approach to cosmological correlators. While some partial results in this direction have been found [1–19]—

notably the “cosmological polytopes” associated with a new combinatorial/geometric understanding of the flat-space wavefunction [20–22]—we have not yet seen a single example of a completely “autonomous” set of ideas for determining the cosmological wavefunction, purely in terms of the kinematic data specifying the observable itself, capturing the dynamics of “bulk” time evolution in purely “boundary” terms.

Our goal in this Letter is to change this state of affairs. We will study an evolution in the space of kinematic configurations—called *kinematic flow*—that replaces the ordinary notion of cosmological time evolution. Remarkably, this flow can be defined autonomously in the space of boundary kinematics, and a few simple rules allow us to predict the differential equations for arbitrary tree graphs (at least in a toy model of cosmological evolution).

Boundary kinematics. We describe cosmological fluctuations in Fourier space, where the kinematic data is a set of wavevectors (momenta) \vec{k}_a , which form a closed polygon as a consequence of momentum conservation:



Correlators are then functions of the lengths of the sides and diagonals of these kinematic polygons.

Certain kinematic configurations are special. First, we can analytically continue the side lengths, so that the perimeters of some sub-polygons (including the full polygon) vanish. As we will see, cosmological correlators have singularities at these locations [2, 20, 23]. It will be illuminating to represent these energy singularities graphi-

cally by shading the relevant sub-polygons, such as

$$\begin{array}{|c|} \hline \square \\ \hline \end{array} = k_{1234}, \quad \begin{array}{|c|} \hline \square \\ \hline \end{array} = k_{12} + s, \quad (1)$$

where $k_{n_1 \dots n_j} \equiv |\vec{k}_{n_1}| + \dots + |\vec{k}_{n_j}|$ and $s \equiv |\vec{k}_1 + \vec{k}_2|$. Correlators can, in principle, also have singularities when the sum of some external edges become collinear with a diagonal. We represent this by the following shading

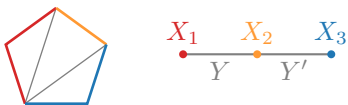
$$\begin{array}{|c|} \hline \square \\ \hline \end{array} = k_{12} - s, \quad (2)$$

where the dashed line indicates that the sign of the internal line is flipped when computing the perimeter.

Graphs and tubings. It is useful to introduce a bit of extra structure in kinematic space. Polygons beg to be triangulated, and so we will pick a particular triangulation of the kinematic polygon. Any triangulation of a polygon has an associated dual graph that encodes the adjacency of triangles. For example, triangulations of the square correspond to graphs with two vertices



where $X_1 \equiv k_{12}$, $X_2 \equiv k_{34}$ and $Y \equiv |\vec{k}_1 + \vec{k}_2|$. Higher-point triangulations have similar representations, such as



where each vertex is associated to a triangle in the triangulation of the pentagon.

Above we described how the singularities of correlators are related to the perimeters of sub-polygons. This also has a useful representation on the dual graph. We first decorate the graph with *markings* (crosses on internal lines), and then draw connected *tubes* (circlings of the vertices and crosses) of these marked graphs. To each tubing, we then assign the sum of vertex energies enclosed by the tube and the energies of the internal lines piercing the tube. For tubes that intersect an internal line and enclose the corresponding cross, we flip the sign of the internal energy. For example, the singularities shown in (1) and (2) correspond to

$$\begin{array}{|c|} \hline \bullet \\ \hline \end{array} \equiv \begin{array}{|c|} \hline \square \\ \hline \end{array}, \quad \begin{array}{|c|} \hline \bullet \\ \hline \end{array} \equiv \begin{array}{|c|} \hline \square \\ \hline \end{array}, \quad \begin{array}{|c|} \hline \bullet \\ \hline \end{array} \equiv \begin{array}{|c|} \hline \square \\ \hline \end{array}.$$

These marked graphs and tubings will play an important role in the construction of differential equations.

Differential equations. The kinematic space of correlations can be expressed in terms of either a polygon or a marked graph. But these are completely static objects, how do they capture actual cosmological correlations? The most basic question we can ask is how the strength

of correlations changes as we vary the external energies (i.e. the shape of the polygon) infinitesimally. This is a differential question, and so we should expect that the answer is captured by a differential equation. What is more remarkable is that these differential equations can also be understood as arising from a sort of flow through the space of graph tubings.

We denote the correlation function associated to a kinematic graph by ψ . We then take derivatives of ψ with respect to the energies Z_I (which includes both the external energies X_i and the exchange energies Y_j). Generically, this will generate new functions (and possibly the function ψ itself). Differentiating these functions, produces additional new functions, and so on. A priori there is no reason that this procedure should ever terminate, but in our case it will. We therefore have a finite basis of functions S_a , and can assemble them into a vector $\vec{I} \equiv (\psi, S_1, \dots, S_{n-1})^T$. Since the system is finite, it must satisfy a differential equation of the form

$$d\vec{I} = A\vec{I}, \quad (3)$$

where A is a matrix-valued one-form and we have defined the total differential $d \equiv \sum_I \partial_{Z_I} dZ_I$.

The challenge now is to generate the connection matrix A . In the following, we will describe a combinatorial procedure that accomplishes this task in terms of a *kinematic flow* through the space of (marked) graph tubings. The output of this procedure will be a connection of the form

$$A = \sum_i \alpha_i d \log \Phi_i(Z), \quad (4)$$

where α_i are constant matrices and $\Phi_i(Z)$ are the *letters* of the differential equation. Notably, this equation is a sum of dlog forms and thus is Abelian flat ($dA = 0$).

Conceptually, there are three ingredients to the equation (3). First, we have to enumerate the possible letters that can appear in the connection matrix (4). Next, we have to determine how many functions appear in the vector \vec{I} , and organize them in some way. Finally, we need a way to derive the differential of \vec{I} , and hence obtain the coefficient matrices α_i . We will address each of these needs in turn.

Letters. We start by describing the possible singularities of the differential equations (i.e. its letters). They are naturally encoded by the same graph tubings that we introduced to label kinematic limits. For example, the letters (represented as dlog forms) of the two-site chain are the following tubings of the marked graph:

$$\begin{array}{|c|} \hline \bullet \\ \hline \end{array} \equiv d \log(X_1 + Y), \quad \begin{array}{|c|} \hline \bullet \\ \hline \end{array} \equiv d \log(X_1 - Y), \\ \begin{array}{|c|} \hline \bullet \\ \hline \end{array} \equiv d \log(X_2 + Y), \quad \begin{array}{|c|} \hline \bullet \\ \hline \end{array} \equiv d \log(X_2 - Y), \\ \begin{array}{|c|} \hline \bullet \\ \hline \end{array} \equiv d \log(X_1 + X_2).$$

Starting at three sites, vertices can connect to multiple

lines, leading to letters with multiple sign flips, such as

$$\begin{aligned} \bullet \text{---} \text{---} \text{---} \bullet &\equiv d \log(X_2 - Y + Y'), \\ \bullet \text{---} \text{---} \text{---} \bullet &\equiv d \log(X_2 - Y - Y'). \end{aligned}$$

In total, there are 13 letters for the three-site graph.

Functions. Next, we define the set of basis functions of the differential equation. For this purpose, we introduce a second type of graph tubings. This time, we draw all “complete tubings” of the graph (non-nested and non-intersecting tubings that enclose all vertices). Each tubing corresponds to a unique basis function. Tubings that contain at least one cross are associated to source functions, while the wavefunction itself has no enclosed crosses. For the two-site chain, the set of functions is

$$\begin{array}{ccc} \psi \text{---} \text{---} \bullet & F \text{---} \text{---} \bullet & Z \text{---} \text{---} \bullet \\ & \tilde{F} \text{---} \text{---} \bullet & \end{array}$$

while, for the three-site chain, we have

$$\begin{array}{ccc} \psi \text{---} \text{---} \bullet & f \text{---} \text{---} \bullet & g \text{---} \text{---} \bullet \\ F \text{---} \text{---} \bullet & q_1 \text{---} \text{---} \bullet & \tilde{g} \text{---} \text{---} \bullet \\ \tilde{F} \text{---} \text{---} \bullet & q_2 \text{---} \text{---} \bullet & Z \text{---} \text{---} \bullet \\ Q_1 \text{---} \text{---} \bullet & q_3 \text{---} \text{---} \bullet & \\ Q_2 \text{---} \text{---} \bullet & \tilde{q}_1 \text{---} \text{---} \bullet & \\ Q_3 \text{---} \text{---} \bullet & \tilde{q}_2 \text{---} \text{---} \bullet & \\ & \tilde{q}_3 \text{---} \text{---} \bullet & \end{array}$$

Here, we have ordered the graphs by the number of vertices enclosed by tubes that also contain a cross.

Kinematic flow. The final ingredients are the coefficient matrices α_i in (4). In the following, we introduce a set of *rules* that dictate how the graph tubings associated to the basis functions “evolve” when we take derivatives. This will allow us to write down—by hand—the differential equations for all tree graphs.

We start with the tubing associated to a “parent function” of interest and then generate a “family tree” of its “descendants” according to a set of rules, from which we can then read off the differential of the parent function. The procedure is best illustrated by an example, and a particularly instructive case is the function Q_1 of the three-site chain:

1. *Activation*—We first move through the graph and “activate” each tube enclosing a vertex. Each activation forms a branch of the tree.

For the function Q_1 , we generate

$$\begin{array}{c} \bullet \text{---} \text{---} \bullet \\ \swarrow \quad \downarrow \quad \searrow \\ \bullet \text{---} \text{---} \bullet \quad \bullet \text{---} \text{---} \bullet \quad \bullet \text{---} \text{---} \bullet \end{array} \quad (5)$$

where the colored tubes are activated in each branch.

2. *Growth*—Activated tubes with no crosses can “grow” to enclose adjacent crosses in all possible ways. For example, in the bottom branch of (5), we have

$$\bullet \text{---} \text{---} \bullet \rightarrow \bullet \text{---} \text{---} \bullet \quad (6)$$

3. *Merger*—If a grown tube intersects another tube, they “merge” (i.e. their union becomes activated). Such a merger occurs in the top branch of (5):

$$\bullet \text{---} \text{---} \bullet \rightarrow \bullet \text{---} \text{---} \bullet \quad (7)$$

where $\bullet \text{---} \text{---} \bullet \Rightarrow \bullet \text{---} \text{---} \bullet$. Tubes that grow/merge lead to additional descendant layers in the tree.

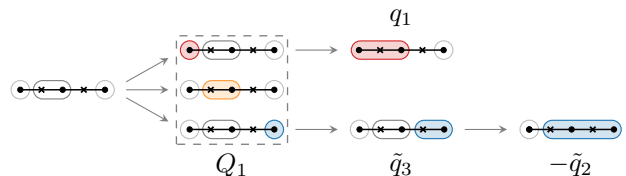
4. *Absorption*—If an activated tube is adjacent to another tube with a cross, it further merges with this tube (“absorbs” it). This absorption is directional and only occurs if the cross in the activated tube points in the direction of the other tube. Absorption again generates an additional level of the tree.

For the function Q_1 , such an absorption happens once:

$$\bullet \text{---} \text{---} \bullet \rightarrow \bullet \text{---} \text{---} \bullet \quad (8)$$

(Note there is no absorption for $\bullet \text{---} \text{---} \bullet$ in (5), because the adjacent non-active tube does not contain a cross.)

Combining the above elements, the complete family tree for the function Q_1 is



To each graph in the tree, we assigned the function corresponding to the graph tubing (ignoring whether tubes are active or not). The sign of each descendant function is determined by the number of absorptions along the path from the original parent graph. We pick up a minus sign for each absorption. (This is why the function \tilde{q}_2 above comes with a minus sign.) If an activated tube at the first level contains more than one vertex, we multiply the corresponding function by the number of enclosed vertices (see Appendix A for an example).

Given a family tree like the one above, it is then simple to write down the differential of the parent function:

1. For each graph in the tree, write the $d \log$ of the letter associated to the active tube.
2. Multiply this letter by the function associated to the graph *minus* the functions associated to all of its immediate descendant graphs, with an overall constant factor ε .

For the function Q_1 , this procedure gives

$$\begin{aligned} dQ_1 = \varepsilon [& (Q_1 - q_1) \bullet \text{---} \text{---} \bullet + q_1 \bullet \text{---} \text{---} \bullet \\ & + Q_1 \bullet \text{---} \text{---} \bullet \\ & + (Q_1 - \tilde{q}_3) \bullet \text{---} \text{---} \bullet + (\tilde{q}_3 + \tilde{q}_2) \bullet \text{---} \text{---} \bullet \\ & - \tilde{q}_2 \bullet \text{---} \text{---} \bullet]. \end{aligned} \quad (9)$$

The overall factor of ε normalizes the residues of the singularities. Later, we will see that this is related to the evolution of the scale factor in a power-law cosmology.

We have presented the simplest example which still displays all the important qualitative features. Of course, in more complicated graphs, repeated application of these steps can lead to more complex phenomena. For example, if an activated tube is connected to multiple internal lines it can grow in multiple directions (see Appendix A). Similarly, multiple absorptions can occur either at the same time or sequentially [24].

A critical feature of the kinematic flow rules is that they imply $d^2 = 0$ acting on any function, so that the equations are compatible. This requires a nontrivial interplay between the procedure itself (the subtraction of functions and assignment of signs) and linear relations between the kinematic letters that imply that certain combinations of $d \log$ forms vanish [24].

Examples. Remarkably, the preceding algorithm can be used to generate the system of differential equations associated to arbitrary tree graphs. For example, the system satisfied by the two-site chain is

$$d\psi = \varepsilon \left[(\psi - F) \begin{array}{c} \circ \leftarrow \bullet \\ \bullet \leftarrow \circ \end{array} + (\psi - \tilde{F}) \begin{array}{c} \bullet \leftarrow \circ \\ \circ \leftarrow \bullet \end{array} + F \begin{array}{c} \bullet \leftarrow \bullet \\ \bullet \leftarrow \bullet \end{array} + \tilde{F} \begin{array}{c} \bullet \leftarrow \bullet \\ \bullet \leftarrow \bullet \end{array} \right] \quad (10)$$

$$dF = \varepsilon \left[F \begin{array}{c} \bullet \leftarrow \bullet \\ \bullet \leftarrow \bullet \end{array} + (F - Z) \begin{array}{c} \bullet \leftarrow \bullet \\ \bullet \leftarrow \bullet \end{array} + Z \begin{array}{c} \bullet \leftarrow \bullet \\ \bullet \leftarrow \bullet \end{array} \right] \quad (11)$$

$$d\tilde{F} = \varepsilon \left[\tilde{F} \begin{array}{c} \bullet \leftarrow \bullet \\ \bullet \leftarrow \bullet \end{array} + (\tilde{F} - Z) \begin{array}{c} \bullet \leftarrow \bullet \\ \bullet \leftarrow \bullet \end{array} + Z \begin{array}{c} \bullet \leftarrow \bullet \\ \bullet \leftarrow \bullet \end{array} \right] \quad (12)$$

$$dZ = 2\varepsilon Z \begin{array}{c} \bullet \leftarrow \bullet \\ \bullet \leftarrow \bullet \end{array} \quad (13)$$

We can see the features of the flow through kinematic space in these equations. The differential of ψ generates source functions F, \tilde{F} , which themselves are sourced by Z , and which are associated to the growth of a tubing on the graph associated to the kinematic variables.

In Appendix A, we present the complete set of equations for the three-site chain. Examples of longer chains and more complicated graph topologies can be found in [24]. The crucial point is that the equations for larger graphs become very complicated, but the rules for generating these equations remain simple.

Emergent time. So far, the function ψ has been a purely mathematical object, and we have not yet connected it to physics. Remarkably, ψ has an interpretation as the wavefunction coefficient for a conformally coupled scalar in an FRW cosmology, with the scale factor $a(\eta) \propto \eta^{-(1+\varepsilon)}$ [20]. One way to see this is to recast the output of a bulk calculation in a form where the system of equations like (10)–(13) can be derived and all of the basis functions can be given a bulk interpretation [24]. However, showing this explicitly would take us too far afield, so instead we will just give a glimpse of the encoding of time evolution by the differential equations.

From the general structure of the equations (10)–(13), it is guaranteed that ψ satisfies a fourth-order homogeneous differential equation (since the basis is four-dimensional and each function satisfies a first-order equation). However, in the (non-generic) physical situation, two small miracles occur. The wavefunction ψ actually

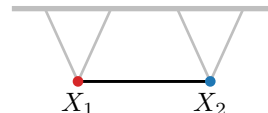
satisfies a second-order inhomogeneous equation (or a third-order homogeneous equation):

$$\square \psi = g(X_1 + X_2)^{-(1-2\varepsilon)}, \quad (14)$$

and the relevant differential operator involves *only* X_1 :

$$\square \equiv (X_1^2 - Y^2) \partial_{X_1}^2 + 2(1 - \varepsilon) X_1 \partial_{X_1} - \varepsilon(1 - \varepsilon), \quad (15)$$

(and similarly for X_2). The nontrivial feature that this equation encodes is that there is a *local* differential operator that simplifies the singularity structure of the wavefunction ψ . This reflects the fact that the wavefunction can equally be thought of as arising from a bulk time integral associated to the Feynman diagram



where the existence of such a differential operator is a consequence of the fact that the bulk-to-bulk propagator satisfies $\square G(x) = i\delta(x)$ [6], where \square is now the d'Alembertian in the bulk spacetime. It is remarkable that by asking a completely static question in the space of kinematic variables, we are led to a function that can equally well be interpreted as coming from cosmological time evolution.

Sum over graphs. So far, we have discussed the differential equations for individual graphs (or specific triangulations of the kinematic polygon). For scattering amplitudes, however, the most stunning simplifications arise in the sum over Feynman graphs [25–29], while the individual graphs are often not even physically meaningful objects. It remains an important open problem to find similar irreducible structures for the cosmological wavefunction that emerge when summing over graphs.

We will see some hints of deeper structure by removing the scaffolding of a choice of triangulation of the kinematic polygon, and instead summing over triangulations. The output will again have a physical interpretation, but now as the (flavor-ordered) wavefunction in $\text{tr } \phi^3$ theory, which involves a sum over planar graphs [30, 31].

A four-point function has two different triangulations



corresponding to s and t -channel exchanges. Similarly, a five-point function is associated to a pentagon, which has five different triangulations



In general, the triangulations of an n -gon are counted by the Catalan numbers C_{n-2} .

The full wavefunction is again a member of a finite space of functions, which satisfy differential equations.

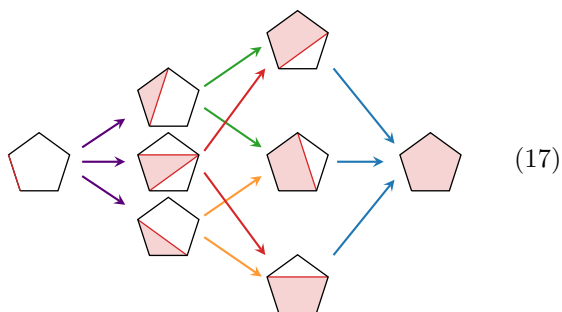
This time, we take derivatives with respect to the external energies k_i (i.e. the side lengths of the kinematic polygon). The letters in the differential equation are now associated to shaded sub-polygons, where we allow internal lines to be either solid or dashed (see above). Similarly, functions are associated to (possibly disconnected) shadings of polyangulations, which are the analogue of the disjoint tubings in the single-graph case.

The kinematic flow now determines the evolution of shaded polyangulations. The precise rules are given in [24]. Here, we will simplify the discussion by restricting ourselves to taking successive partial derivatives with respect to a single edge of the polygon (say the edge corresponding to the energy k_1). The k_1 -derivative of the wavefunction ψ then generates shadings of all triangles that contain the edge associated to k_1 . Internal lines can be solid or dashed. Taking further k_1 -derivatives, the shadings grow by attaching further triangles. For example, in the case of the four-point function, the evolution of shadings is

$$\psi \begin{array}{c} \square \\ \square \end{array} \xrightarrow{\partial_{k_1}} \begin{array}{c} \psi^{(s)} \\ \psi^{(t)} \end{array} \rightarrow \begin{array}{c} F^{(s)} \\ F^{(t)} \end{array} \rightarrow Z \quad (16)$$

There are two different paths for reaching the completely shaded square. The function Z associated to this shading is then “shared” between the s - and t -channel equations.

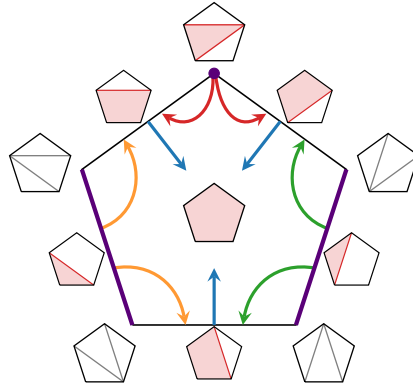
For the four-point function, only one function is shared between channels, but the structure becomes more intricate at higher points [24]. For example, the five-point function has the following sequence of shadings:



To reduce the size of the figure, we have suppressed the solid/dashed distinction of the internal lines. We now see multiple shared functions between the different channels.

A convenient way to visualize the relationship between the functions is to assign them to the geometry of an *associahedron*. To each vertex of the associahedron, we attach a complete triangulation of the kinematic polygon (and hence functions that are unique to the different channels), while the facets of the geometry correspond to partial triangulations (and hence shared functions). For

the case of the five-point function, we have



Shown here are the shadings appearing in (17). We have also indicated how the shadings evolve along the associahedron under the kinematic flow. Other shadings would appear if we were to take derivatives with respect to the other energies (and not just k_1). In general, we can think of the associahedron as being dressed with the basis functions and letters corresponding to the (partial) triangulations on its facets and vertices. For the five-point function, there are 7 functions associated to each vertex, 4 shared functions at each edge and 1 shared function on the face of the pentagon [24].

Outlook. In this Letter, we introduced simple and universal rules underlying the apparent complexity of the differential equations for the FRW wavefunction of conformally coupled scalars. These rules govern a flow in the boundary kinematic space and make no explicit reference to time evolution in the bulk spacetime. It is intriguing that the components of the construction appear naturally in the kinematic space of cosmological correlators, and are related to interesting combinatorial objects.

We motivated this endeavor as the search for a viewpoint where time is a derived concept. To view this as a true emergence of time, however, requires that this kinematic flow takes on a life of its own, by being derived from a different set of physical and mathematical principles. The mere existence of this structure is already a hint that a more elemental formulation exists, and we have seen glimpses of such hidden magic. We hope that this work serves as inspiration for finding the deeper mathematical structure underlying cosmological correlations.

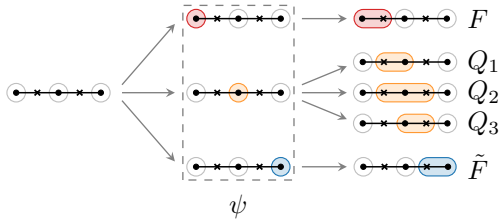
Acknowledgements: We are grateful for feedback and discussions to Ana Achúcarro, Paolo Benincasa, Jan de Boer, Alessandra Caraceni, J. J. Carrasco, Xingang Chen, Claude Duhr, Alex Edison, Carolina Figueiredo, Dan Green, Thomas Grimm, Song He, Johannes Henn, Arno Hoefnagels, Yu-tin Huang, Michael Jones, Manki Kim, Barak Kol, Chia-Kai Kuo, Daniel Longenecker, Manuel Loparco, Scott Melville, Sebastian Mizera, Matteo Parisi, Julio Parra-Martinez, Nic Pavao, Andrzej Pokraka, Oliver Schlotterer, Leonardo Senatore, Chia-Hsien Shen, John Stout, Bernd Sturmfels, Simon Telen, Jaroslav Trnka, Kamran Salehi Vaziri, Dong-Gang Wang and Alexander Zhiboedov.

NAH is supported by the US Department of Energy (DOE) under contract DE-SC0009988. DB is supported by a Yushan Professorship at National Taiwan University funded by the Ministry of Education (Taiwan). AH is supported by DOE (HEP) Award DE-SC0011632 and by the Walter Burke Institute for Theoretical Physics. AJ is supported in part by DOE (HEP) Award DE-SC0009924. HL is supported by the Kavli Institute for Cosmological Physics at the University of Chicago through an endowment from the Kavli Foundation and its founder Fred Kavli. GLP is supported by a Rita-Levi Montalcini fellowship from the Italian Ministry of Universities and Research (MUR) and by INFN (IS GSS-Pi).

Appendix A: Equations for the Three-Site Chain

In this appendix, we will use the rules of the kinematic flow to derive the complete set of differential equations satisfied by the basis functions of the three-site chain.

Level 1: The equation of the wavefunction is given by the following evolutionary tree:



We see that there are three ways in which the middle tube can grow to encircle the neighboring crosses. This produces the three source functions $Q_{1,2,3}$. From this tree, we infer the following differential

$$d\psi = \varepsilon \left[(\psi - F) \begin{array}{c} \circ \\ \bullet \end{array} \begin{array}{c} \bullet \\ \circ \end{array} \begin{array}{c} \bullet \\ \bullet \\ \bullet \end{array} + (\psi - \sum Q_i) \begin{array}{c} \bullet \\ \bullet \\ \bullet \end{array} \begin{array}{c} \circ \\ \bullet \\ \circ \end{array} \begin{array}{c} \bullet \\ \bullet \\ \bullet \end{array} \right. \\ \left. + F \begin{array}{c} \bullet \\ \bullet \\ \bullet \end{array} \begin{array}{c} \bullet \\ \bullet \\ \bullet \end{array} \begin{array}{c} \circ \\ \bullet \\ \bullet \end{array} + Q_1 \begin{array}{c} \bullet \\ \bullet \\ \bullet \end{array} \begin{array}{c} \bullet \\ \bullet \\ \bullet \end{array} \begin{array}{c} \circ \\ \bullet \\ \bullet \end{array} \right. \\ \left. (\psi - \tilde{F}) \begin{array}{c} \bullet \\ \bullet \\ \bullet \end{array} \begin{array}{c} \bullet \\ \bullet \\ \bullet \end{array} \begin{array}{c} \bullet \\ \bullet \\ \circ \end{array} + Q_2 \begin{array}{c} \bullet \\ \bullet \\ \bullet \end{array} \begin{array}{c} \bullet \\ \bullet \\ \bullet \end{array} \begin{array}{c} \bullet \\ \bullet \\ \circ \end{array} \right. \\ \left. + \tilde{F} \begin{array}{c} \bullet \\ \bullet \\ \bullet \end{array} \begin{array}{c} \bullet \\ \bullet \\ \bullet \end{array} \begin{array}{c} \bullet \\ \bullet \\ \circ \end{array} + Q_3 \begin{array}{c} \bullet \\ \bullet \\ \bullet \end{array} \begin{array}{c} \bullet \\ \bullet \\ \bullet \end{array} \begin{array}{c} \bullet \\ \bullet \\ \circ \end{array} \right]$$

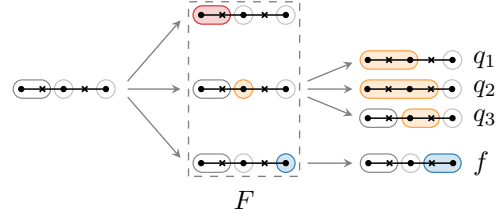
which is similar to (10) for the two-site chain.

Level 2: The differential of ψ involved five source functions, associated to the following graph tubings:

$$\begin{array}{ll} F & \begin{array}{c} \bullet \\ \bullet \\ \bullet \end{array} \begin{array}{c} \bullet \\ \bullet \\ \bullet \end{array} \begin{array}{c} \bullet \\ \bullet \\ \bullet \end{array} \\ \tilde{F} & \begin{array}{c} \bullet \\ \bullet \\ \bullet \end{array} \begin{array}{c} \bullet \\ \bullet \\ \bullet \end{array} \begin{array}{c} \bullet \\ \bullet \\ \circ \end{array} \\ Q_1 & \begin{array}{c} \bullet \\ \bullet \\ \bullet \end{array} \begin{array}{c} \bullet \\ \bullet \\ \bullet \end{array} \begin{array}{c} \bullet \\ \bullet \\ \bullet \end{array} \\ Q_2 & \begin{array}{c} \bullet \\ \bullet \\ \bullet \end{array} \begin{array}{c} \bullet \\ \bullet \\ \bullet \end{array} \begin{array}{c} \bullet \\ \bullet \\ \circ \end{array} \\ Q_3 & \begin{array}{c} \bullet \\ \bullet \\ \bullet \end{array} \begin{array}{c} \bullet \\ \bullet \\ \bullet \end{array} \begin{array}{c} \bullet \\ \bullet \\ \circ \end{array} \end{array}$$

We will now predict the differentials of these functions.

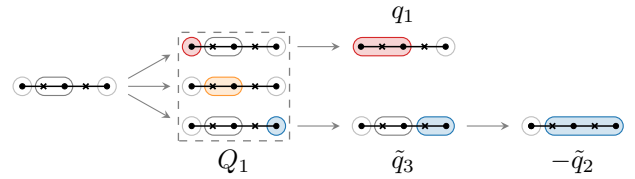
- The differential of the function F is predicted by



Note that the functions q_1 and q_2 are created by mergers, while the functions q_3 and f correspond to disconnected tubings. The differential of F then is

$$dF = \varepsilon \left[F \begin{array}{c} \circ \\ \bullet \end{array} \begin{array}{c} \bullet \\ \circ \end{array} \begin{array}{c} \bullet \\ \bullet \\ \bullet \end{array} + (F - \sum q_i) \begin{array}{c} \bullet \\ \bullet \\ \bullet \end{array} \begin{array}{c} \circ \\ \bullet \\ \circ \end{array} \begin{array}{c} \bullet \\ \bullet \\ \bullet \end{array} \right. \\ \left. + q_1 \begin{array}{c} \bullet \\ \bullet \\ \bullet \end{array} \begin{array}{c} \bullet \\ \bullet \\ \bullet \end{array} \begin{array}{c} \circ \\ \bullet \\ \bullet \end{array} \right. \\ \left. (F - f) \begin{array}{c} \bullet \\ \bullet \\ \bullet \end{array} \begin{array}{c} \bullet \\ \bullet \\ \bullet \end{array} \begin{array}{c} \bullet \\ \bullet \\ \circ \end{array} + q_2 \begin{array}{c} \bullet \\ \bullet \\ \bullet \end{array} \begin{array}{c} \bullet \\ \bullet \\ \bullet \end{array} \begin{array}{c} \bullet \\ \bullet \\ \circ \end{array} \right. \\ \left. + f \begin{array}{c} \bullet \\ \bullet \\ \bullet \end{array} \begin{array}{c} \bullet \\ \bullet \\ \bullet \end{array} \begin{array}{c} \bullet \\ \bullet \\ \circ \end{array} + q_3 \begin{array}{c} \bullet \\ \bullet \\ \bullet \end{array} \begin{array}{c} \bullet \\ \bullet \\ \bullet \end{array} \begin{array}{c} \bullet \\ \bullet \\ \circ \end{array} \right]$$

- The tree for the function Q_1 was presented in the main text. We reproduce it here for completeness:

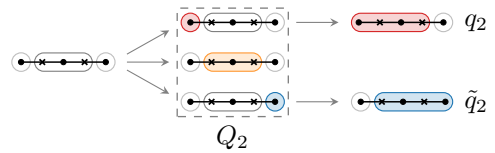


The top branch shows growth and merger, while the bottom branch contains the first instance of the absorption phenomenon. The differential of the function Q_1 then is

$$dQ_1 = \varepsilon \left[(Q_1 - q_1) \begin{array}{c} \circ \\ \bullet \end{array} \begin{array}{c} \bullet \\ \circ \end{array} \begin{array}{c} \bullet \\ \bullet \\ \bullet \end{array} + q_1 \begin{array}{c} \bullet \\ \bullet \\ \bullet \end{array} \begin{array}{c} \bullet \\ \bullet \\ \bullet \end{array} \begin{array}{c} \circ \\ \bullet \\ \bullet \end{array} \right. \\ \left. + Q_1 \begin{array}{c} \bullet \\ \bullet \\ \bullet \end{array} \begin{array}{c} \bullet \\ \bullet \\ \bullet \end{array} \begin{array}{c} \circ \\ \bullet \\ \bullet \end{array} \right. \\ \left. + (Q_1 - \tilde{q}_3) \begin{array}{c} \bullet \\ \bullet \\ \bullet \end{array} \begin{array}{c} \bullet \\ \bullet \\ \bullet \end{array} \begin{array}{c} \bullet \\ \bullet \\ \circ \end{array} \right. \\ \left. + (\tilde{q}_3 + \tilde{q}_2) \begin{array}{c} \bullet \\ \bullet \\ \bullet \end{array} \begin{array}{c} \bullet \\ \bullet \\ \bullet \end{array} \begin{array}{c} \bullet \\ \bullet \\ \circ \end{array} - \tilde{q}_2 \begin{array}{c} \bullet \\ \bullet \\ \bullet \end{array} \begin{array}{c} \bullet \\ \bullet \\ \bullet \end{array} \begin{array}{c} \bullet \\ \bullet \\ \circ \end{array} \right]$$

- By symmetry, the differential for the function Q_3 is equivalent to that of the function Q_1 , and therefore won't be shown explicitly.

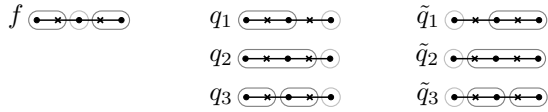
- The tree for the function Q_2 is



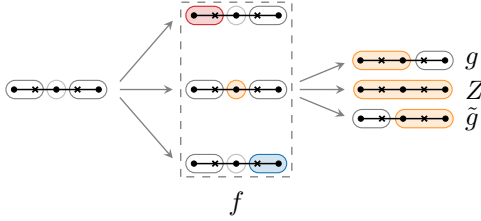
where the functions q_2 and \tilde{q}_2 are created by the standard growth and merger of the tubes. The differential of Q_2 then is

$$dQ_2 = \varepsilon \left[(Q_2 - q_2) \begin{array}{c} \circ \\ \bullet \end{array} \begin{array}{c} \bullet \\ \circ \end{array} \begin{array}{c} \bullet \\ \bullet \\ \bullet \end{array} + q_2 \begin{array}{c} \bullet \\ \bullet \\ \bullet \end{array} \begin{array}{c} \bullet \\ \bullet \\ \bullet \end{array} \begin{array}{c} \circ \\ \bullet \\ \bullet \end{array} \right. \\ \left. + Q_2 \begin{array}{c} \bullet \\ \bullet \\ \bullet \end{array} \begin{array}{c} \bullet \\ \bullet \\ \bullet \end{array} \begin{array}{c} \circ \\ \bullet \\ \bullet \end{array} \right. \\ \left. + (Q_2 - \tilde{q}_2) \begin{array}{c} \bullet \\ \bullet \\ \bullet \end{array} \begin{array}{c} \bullet \\ \bullet \\ \bullet \end{array} \begin{array}{c} \bullet \\ \bullet \\ \circ \end{array} + \tilde{q}_2 \begin{array}{c} \bullet \\ \bullet \\ \bullet \end{array} \begin{array}{c} \bullet \\ \bullet \\ \bullet \end{array} \begin{array}{c} \bullet \\ \bullet \\ \circ \end{array} \right]$$

Level 3: The differentials at Level 2 produced 7 source functions corresponding to the following graph tubings:



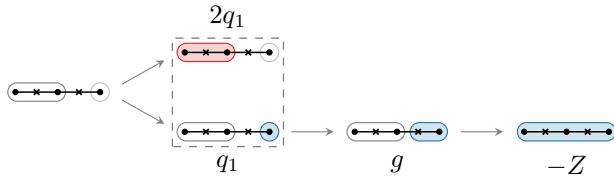
- The tree for the function f is



Note that the function Z is created by the merger of three tubes. The differential of f then is

$$df = \varepsilon \left[f \begin{array}{c} \text{red activation} \\ \text{blue activation} \end{array} + (F - g - \tilde{g} - Z) \begin{array}{c} \text{orange activation} \\ \text{blue activation} \end{array} + g \begin{array}{c} \text{orange activation} \\ \text{blue activation} \end{array} + \tilde{g} \begin{array}{c} \text{orange activation} \\ \text{blue activation} \end{array} + Z \begin{array}{c} \text{orange activation} \\ \text{blue activation} \end{array} \right]$$

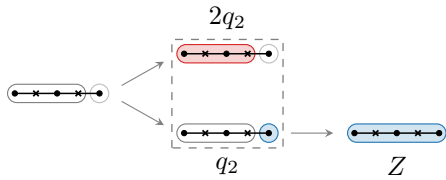
- The tree for the function q_1 is



where we have an instance of growth and absorption in the bottom branch. The assigned function in the top branch comes with a factor of 2 since the activated tube encloses 2 vertices. The differential of q_1 then is

$$dq_1 = \varepsilon \left[2q_1 \begin{array}{c} \text{red activation} \\ \text{blue activation} \end{array} + (q_1 - g) \begin{array}{c} \text{orange activation} \\ \text{blue activation} \end{array} + (g + Z) \begin{array}{c} \text{orange activation} \\ \text{blue activation} \end{array} - Z \begin{array}{c} \text{orange activation} \\ \text{blue activation} \end{array} \right]$$

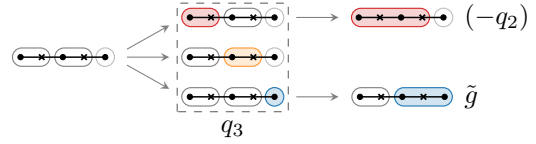
- The tree for the function q_2 is



so that the differential is

$$dq_2 = \varepsilon \left[2q_2 \begin{array}{c} \text{red activation} \\ \text{blue activation} \end{array} + (q_2 - Z) \begin{array}{c} \text{orange activation} \\ \text{blue activation} \end{array} + Z \begin{array}{c} \text{orange activation} \\ \text{blue activation} \end{array} \right]$$

- The tree for the function q_3 is

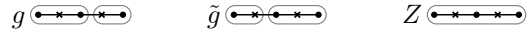


In the top branch, the left tube is first activated and then absorbs its neighboring tube. The remaining features of the tree are the standard activation, growth and merger. The differential of q_3 then is

$$dq_3 = \varepsilon \left[(q_3 + q_2) \begin{array}{c} \text{red activation} \\ \text{orange activation} \end{array} - q_2 \begin{array}{c} \text{red activation} \\ \text{orange activation} \end{array} + q_3 \begin{array}{c} \text{orange activation} \\ \text{blue activation} \end{array} + (q_3 - \tilde{g}) \begin{array}{c} \text{orange activation} \\ \text{blue activation} \end{array} + \tilde{g} \begin{array}{c} \text{orange activation} \\ \text{blue activation} \end{array} \right]$$

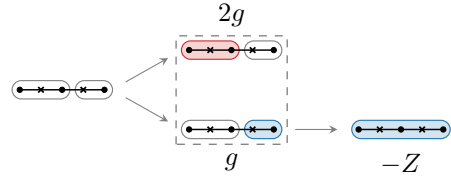
- The differentials for $\tilde{q}_{1,2,3}$ are related to those of $q_{1,2,3}$ by symmetry and are therefore not shown explicitly.

Level 4: At Level 3, we obtained three new source functions corresponding to the following graph tubings:



To complete our analysis, we consider their differentials.

- The tree for the function g is



which is similar to the tree for q_2 , except that the function Z is created by absorption (rather than merger) and therefore comes with a minus sign. The differential of g then is

$$dg = \varepsilon \left[2g \begin{array}{c} \text{red activation} \\ \text{blue activation} \end{array} + (g + Z) \begin{array}{c} \text{orange activation} \\ \text{blue activation} \end{array} - Z \begin{array}{c} \text{orange activation} \\ \text{blue activation} \end{array} \right]$$

- The differential for the function \tilde{g} is related to that of the function g by symmetry and therefore is not shown explicitly.

- Finally, the tree for the function Z is



The tube is simply activated and the assigned coefficient function is 3 times the original function (since the activated tube contains 3 vertices). The differential of Z then is

$$dZ = 3\varepsilon Z \begin{array}{c} \text{green activation} \end{array}$$

We have seen that all equations for the three-site chain are predicted by the simple rules of the kinematic flow. In fact, as we show in our companion paper [24], the same rules underly the equations for arbitrary tree graphs.

-
- [1] D. Baumann, D. Green, A. Joyce, E. Pajer, G. Pimentel, C. Sleight, and M. Taronna, Snowmass White Paper: The Cosmological Bootstrap, in *Snowmass Summer Study*, [arXiv:2203.08121 \[hep-th\]](#).
- [2] J. Maldacena and G. Pimentel, On Graviton Non-Gaussianities during Inflation, *JHEP* **09**, 045, [arXiv:1104.2846 \[hep-th\]](#).
- [3] I. Mata, S. Raju, and S. Trivedi, CMB from CFT, *JHEP* **07**, 015, [arXiv:1211.5482 \[hep-th\]](#).
- [4] P. McFadden and K. Skenderis, Holography for Cosmology, *Phys. Rev. D* **81**, 021301 (2010), [arXiv:0907.5542 \[hep-th\]](#).
- [5] A. Bzowski, P. McFadden, and K. Skenderis, Implications of Conformal Invariance in Momentum Space, *JHEP* **03**, 111, [arXiv:1304.7760 \[hep-th\]](#).
- [6] N. Arkani-Hamed and J. Maldacena, Cosmological Collider Physics, (2015), [arXiv:1503.08043 \[hep-th\]](#).
- [7] N. Arkani-Hamed, D. Baumann, H. Lee, and G. Pimentel, The Cosmological Bootstrap: Inflationary Correlators from Symmetries and Singularities, *JHEP* **04**, 105, [arXiv:1811.00024 \[hep-th\]](#).
- [8] D. Baumann, C. Duaso Pueyo, A. Joyce, H. Lee, and G. Pimentel, The Cosmological Bootstrap: Weight-Shifting Operators and Scalar Seeds, *JHEP* **12**, 204, [arXiv:1910.14051 \[hep-th\]](#).
- [9] D. Baumann, C. Duaso Pueyo, A. Joyce, H. Lee, and G. Pimentel, The Cosmological Bootstrap: Spinning Correlators from Symmetries and Factorization, *SciPost Phys.* **11**, 071 (2021), [arXiv:2005.04234 \[hep-th\]](#).
- [10] C. Sleight, A Mellin Space Approach to Cosmological Correlators, *JHEP* **01**, 090, [arXiv:1906.12302 \[hep-th\]](#).
- [11] C. Sleight and M. Taronna, Bootstrapping Inflationary Correlators in Mellin Space, *JHEP* **02**, 098, [arXiv:1907.01143 \[hep-th\]](#).
- [12] E. Pajer, Building a Boostless Bootstrap for the Bispectrum, *JCAP* **01**, 023, [arXiv:2010.12818 \[hep-th\]](#).
- [13] H. Goodhew, S. Jazayeri, and E. Pajer, The Cosmological Optical Theorem, *JCAP* **04**, 021, [arXiv:2009.02898 \[hep-th\]](#).
- [14] S. Jazayeri, E. Pajer, and D. Stefanyszyn, From Locality and Unitarity to Cosmological Correlators, *JHEP* **10**, 065, [arXiv:2103.08649 \[hep-th\]](#).
- [15] L. Di Pietro, V. Gorbenko, and S. Komatsu, Analyticity and Unitarity for Cosmological Correlators, *JHEP* **03**, 023, [arXiv:2108.01695 \[hep-th\]](#).
- [16] M. Hogervorst, J. Penedones, and K. S. Vaziri, Towards the Non-Perturbative Cosmological Bootstrap, *JHEP* **02**, 162, [arXiv:2107.13871 \[hep-th\]](#).
- [17] G. Pimentel and D.-G. Wang, Boostless Cosmological Collider Bootstrap, *JHEP* **10**, 177, [arXiv:2205.00013 \[hep-th\]](#).
- [18] S. Jazayeri and S. Renaux-Petel, Cosmological bootstrap in slow motion, *JHEP* **12**, 137, [arXiv:2205.10340 \[hep-th\]](#).
- [19] D.-G. Wang, G. Pimentel, and A. Achúcarro, Bootstrapping Multi-Field Inflation: Non-Gaussianities from Light Scalars Revisited, *JCAP* **05**, 043, [arXiv:2212.14035 \[astro-ph.CO\]](#).
- [20] N. Arkani-Hamed, P. Benincasa, and A. Postnikov, Cosmological Polytopes and the Wavefunction of the Universe, (2017), [arXiv:1709.02813 \[hep-th\]](#).
- [21] P. Benincasa, From the Flat-Space S-matrix to the Wavefunction of the Universe, (2018), [arXiv:1811.02515 \[hep-th\]](#).
- [22] P. Benincasa, Cosmological Polytopes and the Wavefunction of the Universe for Light States, (2019), [arXiv:1909.02517 \[hep-th\]](#).
- [23] S. Raju, New Recursion Relations and a Flat Space Limit for AdS/CFT Correlators, *Phys. Rev. D* **85**, 126009 (2012), [arXiv:1201.6449 \[hep-th\]](#).
- [24] N. Arkani-Hamed, D. Baumann, A. Hillman, A. Joyce, H. Lee, and G. Pimentel, Differential Equations for Cosmological Correlators (to appear).
- [25] S. Parke and T. Taylor, An Amplitude for n Gluon Scattering, *Phys. Rev. Lett.* **56**, 2459 (1986).
- [26] P. Benincasa and F. Cachazo, Consistency Conditions on the S-Matrix of Massless Particles, (2007), [arXiv:0705.4305 \[hep-th\]](#).
- [27] A. Hodges, A Simple Formula for Gravitational MHV Amplitudes, (2012), [arXiv:1204.1930 \[hep-th\]](#).
- [28] C. Cheung, K. Kampf, J. Novotny, and J. Trnka, Effective Field Theories from Soft Limits of Scattering Amplitudes, *Phys. Rev. Lett.* **114**, 221602 (2015), [arXiv:1412.4095 \[hep-th\]](#).
- [29] N. Arkani-Hamed, Y. Bai, S. He, and G. Yan, Scattering Forms and the Positive Geometry of Kinematics, Color and the Worldsheet, *JHEP* **05**, 096, [arXiv:1711.09102 \[hep-th\]](#).
- [30] F. Cachazo, S. He, and E. Yuan, Scattering of Massless Particles: Scalars, Gluons and Gravitons, *JHEP* **07**, 033, [arXiv:1309.0885 \[hep-th\]](#).
- [31] N. Arkani-Hamed, H. Frost, G. Salvatori, P.-G. Plamondon, and H. Thomas, All Loop Scattering as a Counting Problem, (2023), [arXiv:2309.15913 \[hep-th\]](#).